

HiSST: 4th International Conference on High-Speed Vehicle Science Technology 22 -26 September 2025, Tours, France



Flow Characteristics Verification Experiments of Circular to Obround **Shape Transition Nozzle**

Su-Wan Choi*1, Min-Seon Jo1, Bu-Kyeng Sung1, Si-Yoon Kang1 and Jeong-Yeol Choi?

Abstract

This study presents the design and experimental verification of a Circular-to-Obround Shape Transition (COST) nozzle, proposed as a candidate configuration for scramjet combustors. Conventional scramjets are generally based on either axisymmetric or rectangular cross-sections, each with distinct advantages and drawbacks. Axisymmetric geometries provide structural efficiency and stable pseudo-shock behavior, while rectangular geometries facilitate effective mixing, visualization, and injector placement but suffer from stronger boundary-layer effects and higher total pressure losses. To combine these advantages, an obround cross-section, composed of semicircular arcs and flat walls, was introduced as a novel alternative. The COST nozzle was designed to simulate high-altitude flight conditions, with exit Mach number 2 and static pressure 3 bar at the isolator entrance. Boundary-layer corrections were incorporated using Sivell's method. Experimental validation was performed by connecting the nozzle to the Vitiated Air Heater (VAH) facility at Pusan National University. Cold-flow wedge tests with highspeed Schlieren imaging confirmed uniform exit flow, with measured Mach numbers slightly above the design value due to boundary-layer effects. The results demonstrate the feasibility of the COST nozzle and provide reference data for future investigations of obround scramjet isolator and combustor flow characteristics.

Keywords: Scramjet, Supersonic Flow, Shape Transition Nozzle, Nozzle Design

Nomenclature

Latin

M - Mach number

P – Nozzle upstream pressure

h – Height from testbed to nozzle exit point

(mm) Greek

 β – Shock wave angle (deg)

y – Specific heat ratio

 θ – Flow deflection angle (deg)

Subscripts

1 – Upstream of the shock

calc - Calculated value

1. Introduction

Scramjet combustors have generally been designed based on either axisymmetric or rectangular

HiSST-2025-0150 Page | 1 Flow Characteristics Verification Experiments of Circular to Obround Shape Transition Nozzle Copyright © 2025 by author(s)

¹ Graduate Research Assistant, Pusan National University, Busan 46241, Republic of Korea

² Professor, Pusan National University, Busan 46241, Republic of Korea, <u>aerochoi@pusan.ac.kr</u> (Corresponding)

flowpaths. The choice of geometry depends on the stage of research: rectangular configurations are often adopted for fundamental flow analysis or small-scale experiments, whereas axisymmetric designs are more common in engine development considering integration with actual flight vehicles.[1,2] The two geometries exhibit distinct flow characteristics due to differences in cross-sectional shape. For example, in axisymmetric flowpaths, the combustor wall is continuous, and pseudo-shocks are maintained in a relatively stable and symmetric manner due to axisymmetric acoustic boundary conditions. In contrast, rectangular flowpaths produce asymmetric pseudo-shocks, and total pressure losses can be more significant because of boundary layer growth along flat walls and sharp corners.[3]

Previous studies have highlighted distinct advantages and drawbacks of these conventional geometries. Axisymmetric scramjets are known for their structural efficiency and stable pseudo-shock behavior, which can remain symmetric even under significant back-pressure loading[3]. In contrast, rectangular scramjets provide practical benefits such as ease of injector placement and improved flow visualization but are prone to larger total pressure losses and asymmetric pseudo-shock structures due to corner boundary-layer growth[4]. These differences indicate that while each configuration has merits, neither geometry offers an optimal solution for both flow stability and experimental accessibility.

Previous studies have extensively investigated the complex coupling between shocks, boundary layers, and combustion processes in scramjet flowpaths. Choi et al.[5] demonstrated that combustion induced by shock—boundary-layer interaction (SBLI) strongly depends on geometric scaling, highlighting the sensitivity of pseudo-shock stability to flowpath configuration. Building upon this foundation, numerical and experimental efforts have examined the dynamic response of scramjet combustors to unsteady phenomena. For example, Choi et al.[6] reported that combustion/shock-train interactions play a decisive role in dual-mode scramjet operation, directly affecting mode transition and unstart characteristics.

In addition to SBLI-driven instabilities, several studies have focused on combustion dynamics associated with fuel injection and turbulent mixing. Transverse fuel injection has been identified as a key mechanism for enhancing mixing and flameholding in supersonic combustors (Choi et al.[7], Won et al.[8]). Detached-Eddy Simulation (DES) studies further revealed the importance of turbulence–combustion—shock interactions in determining overall combustor performance (Choi et al.[9], Vyasaprasath et al.[10]). Recent investigations have also emphasized low-frequency instabilities and frequency shifting in scramjet combustors (Jeong et al.[11]), as well as combined diagnostic approaches integrating imaging and synchronized pressure data to resolve dynamic combustion behavior (Jeong & Choi[12]).

These prior works collectively suggest that both geometry-induced SBLI and injection-driven turbulent mixing critically govern scramjet stability and performance. Related studies have further extended to performance estimation of RBCC engines (Kim et al.[13]), unsteady simulations of ram accelerator configurations (Choi et al.[14]), and the influence of fuel temperature on supersonic turbulent combustion (Choi et al.[15]). Advanced computational approaches such as hybrid RANS/LES (Shin et al.[16]) and high-resolution studies of supersonic flame structures (Choi et al.[17]) also provide valuable background for analyzing the complex flowfields of scramjet engines. However, most of these investigations have focused on conventional axisymmetric or rectangular flowpaths. Motivated by these findings, the present study introduces the obround cross-section as a potential alternative, with the expectation that it can mitigate corner-induced pressure losses while maintaining favorable conditions for flow uniformity and visualization.

Beyond these conventional shapes, several researchers have explored alternative cross-sections to address the limitations of axisymmetric and rectangular configurations. Kato et al.[18] compared perisymmetric and axisymmetric scramjet isolators and reported that the perisymmetric configuration exhibited an inlet unstart threshold approximately 20% lower than the axisymmetric case, indicating greater susceptibility to flow instability. Similarly, Yao et al. [19] investigated elliptic cross-sections and

demonstrated superior fuel—air mixing performance compared to axisymmetric combustors at higher inflow Mach numbers. These studies suggest that non-circular geometries can potentially improve combustion dynamics or mixing efficiency but may introduce new challenges such as increased unstart sensitivity.

In this study, we propose an Obround cross-section scramjet as a new design candidate that incorporates the advantages of both axisymmetric and rectangular geometries. The obround cross-section consists of a combination of semicircular arcs and flat walls, which is expected to reduce total pressure losses at corners compared to rectangular designs, while also providing favorable accessibility for visualization and experimental setups. Since flow studies on obround cross-section scramjets remain limited, experimental or numerical validation is required. Accordingly, our research team has been developing a small-scale supersonic combustion test facility for the fundamental flow analysis of an obround cross-section scramjet. Fig. 1 illustrates the schematic of the rectangular scramjet facility from our previous study[20-24], in which the major components are delineated by dashed boxes. In that work, a Circular-to-Rectangular Shape Transition (CRST) nozzle was employed to realize a rectangular cross-section in the combustor. In the present study, the rectangular cross-section combustor highlighted by the bold purple dashed box in Fig. 1 was replaced with an obround cross-section combustor. To achieve this, a Circular-to-Obround Shape Transition (COST) nozzle was designed, and experiments using the COST nozzle were conducted to verify conformity with the intended exit conditions. The results of this verification are discussed herein.

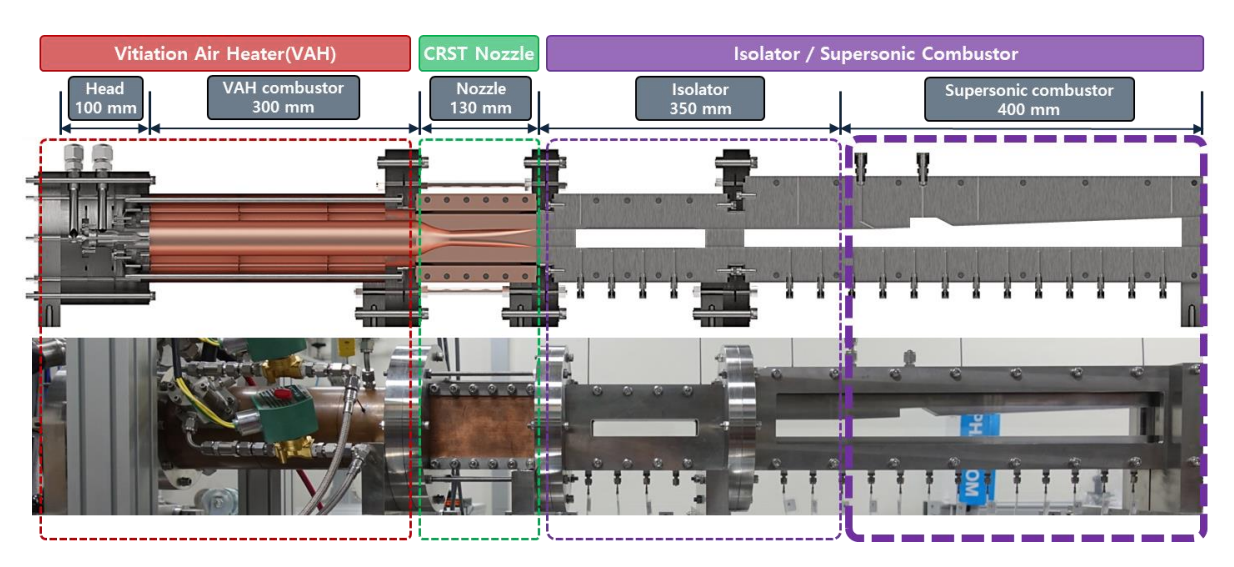


Fig 1. Schematic of the rectangular cross-section scramjet test configuration at Pusan National University [7-14].

2. Experimental Methodology

2.1. Nozzle Design

The COST nozzle was designed to simulate high-altitude conditions at the scramjet isolator entrance, corresponding to a flight Mach number of 6 at an altitude of 30 km. The target isolator inlet condition was set to Mach 2 and a static pressure of 3 bar. The nozzle transitions from a circular throat to an obround cross-section downstream, fully developed at the nozzle exit (Fig. 2).

Upstream of the throat, the geometry follows a conventional converging–diverging nozzle. Downstream, the throat width is maintained at 8.26 mm while developing into an obround shape. The nozzle geometry was designed to achieve an exit Mach number of 2 under $\gamma = 1.4$ conditions, with the

corresponding area ratio set to 1.633. Based on these requirements, the nozzle exit area was determined as 350.38 mm². The nozzle contour was designed using Sivell's method, as in our previous study[22], and corrected for boundary-layer effects. The corrections accounted for momentum and mass deficits, with boundary-layer thickness defined at 99% of the freestream velocity. The corrected contour yielded exit Mach number distributions consistent with Method of Characteristics predictions[23].

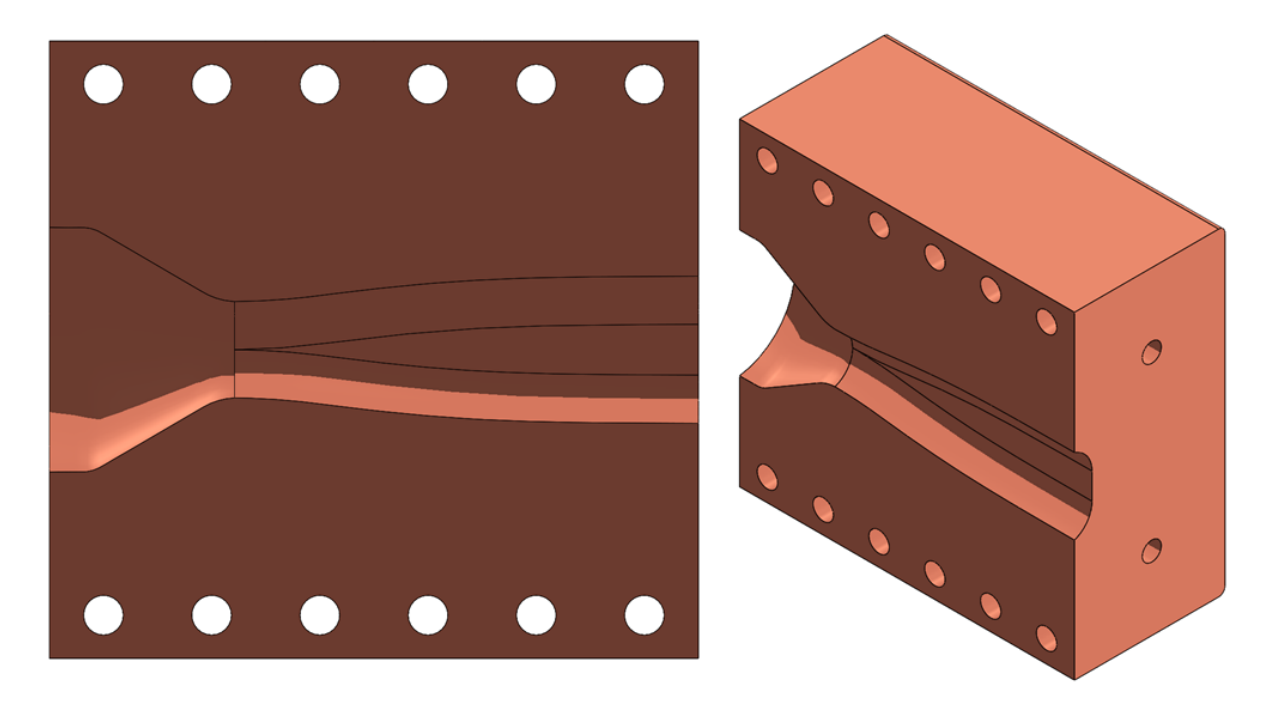


Fig 2. Sectional configuration of Circular to Obround Shape Transition (COST) nozzle.

2.2. Gas Supply, Measurement and Control System

To verify uniformity of the COST nozzle exit, a stable and controllable gas supply system was required to ensure accurate reproduction of the test conditions. Accordingly, the gas supply and control system at Pusan National University was employed. To conduct the cold-flow experiments, a gas supply system capable of delivering gases to the VAH was required. For this purpose, the gas supply system established at Pusan National University was utilized. Fig. 3 shows the piping and instrumentation diagram (P&ID) of the system. This supply system has been experimentally validated through multiple previous studies, and in the present work, only the air gas line was used without combustion.

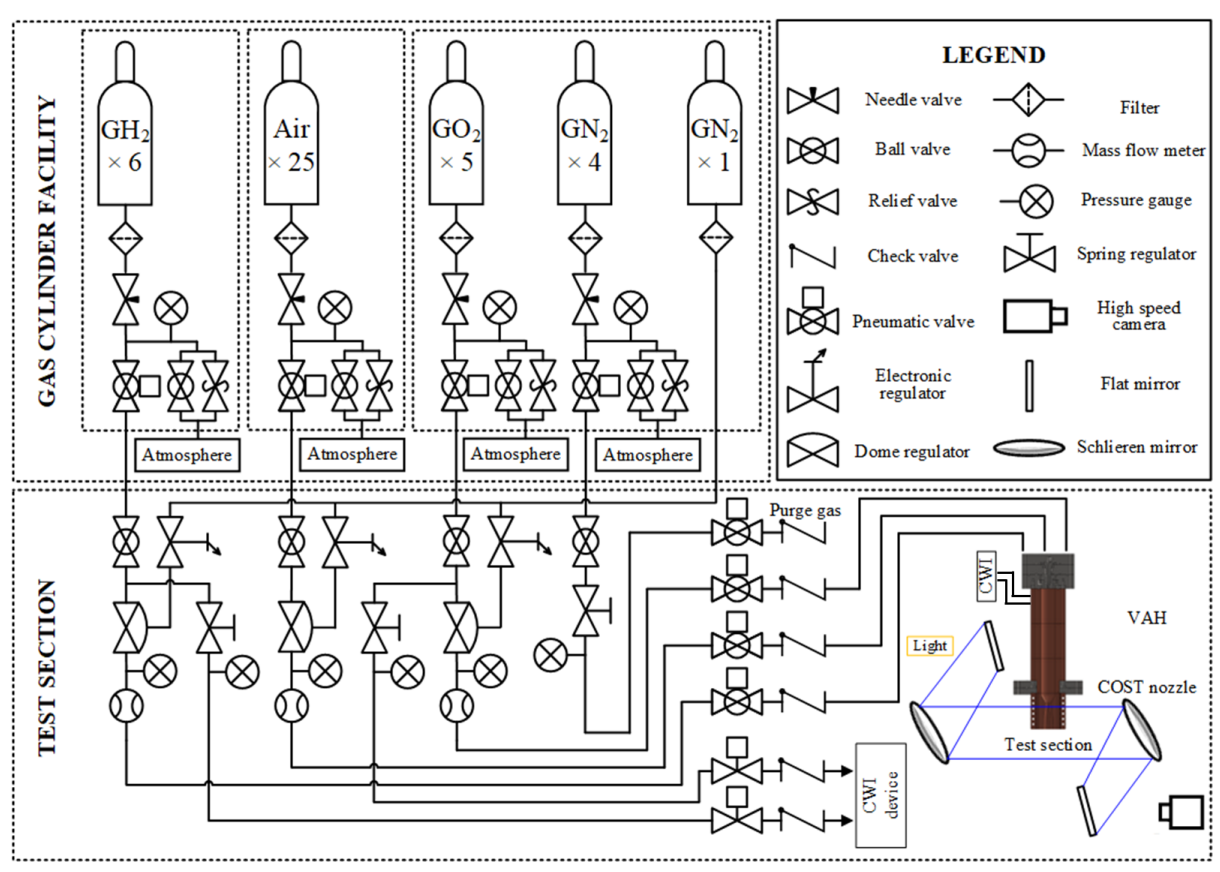
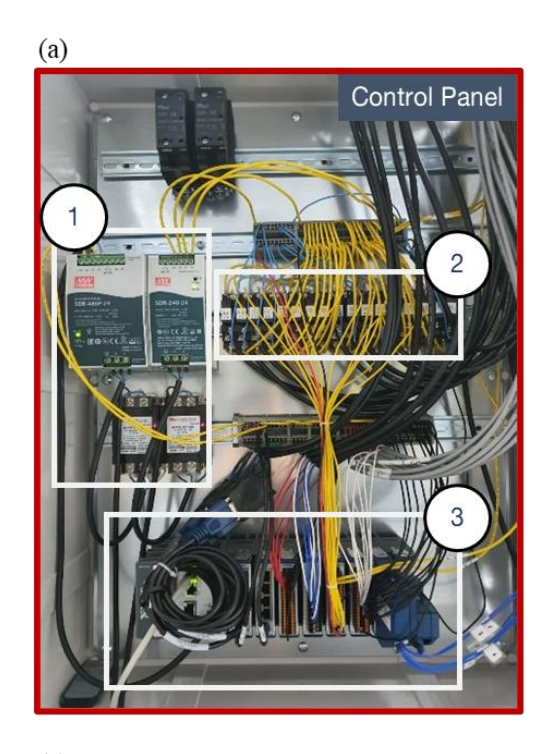


Fig 3. Piping and instrumentation diagram (P&ID) of the gas supply system at Pusan National University.

The pressure required for the cold-flow tests was regulated using dome regulators (Swagelok Inc., RDHN series, Solon, OH). The dome regulators were controlled by electro-pneumatic regulators (ProportionAir Inc., GX series, McCordsville, IN) to set the target pressure. The regulated gas was finally supplied or shut off through pneumatic valves (Swagelok Inc., AT series, Solon, OH), which were installed as close as possible to the VAH. Between the pneumatic valves and the dome regulators, a differential pressure flow meter (Enbac Inc., FM153B, Republic of Korea, <0.2% FS sensor accuracy) was placed to measure the flow rate during gas delivery. The upstream pressure of the COST nozzle was measured at the end of the VAH using a static pressure sensor (WIKA Inc., S-20 series, Germany, >0.5% sensor error).

During the experiments, it was necessary to simultaneously acquire flow rate and upstream pressure data, control the gas supply, and trigger the Schlieren imaging system. For this purpose, the research team employed LabVIEW software (National Instruments) and the NI CompactRIO 9045 module to perform synchronized measurement and control of flow, pressure, and gas supply. Fig. 4 shows the control panel, measurement, and control interface. Fig. 4(a) presents the overall control panel hardware responsible for gas supply control, sensor monitoring, and high-speed camera triggering, while Fig. 4(b) depicts the three main components of the control panel. Component (1), the power supply, provides power to the sensors and pneumatic valves.



- (b)
- Power supply
- ② Solid State Relay
- 3 NI CompactRio 9045 Module

Module	Signal Type	Control	
NI 9871	RS485	Mass flow meter	
NI 9205	Voltage input	Pressure transducer	
NI 9263	Voltage output	Electronic regulator	
NI 9375	Digital I/O	Pneumatic v/v	
NI 9212	Thermocouple input	Thermocouple	
NI 9401	ΠL	High speed camera Scanivalve	

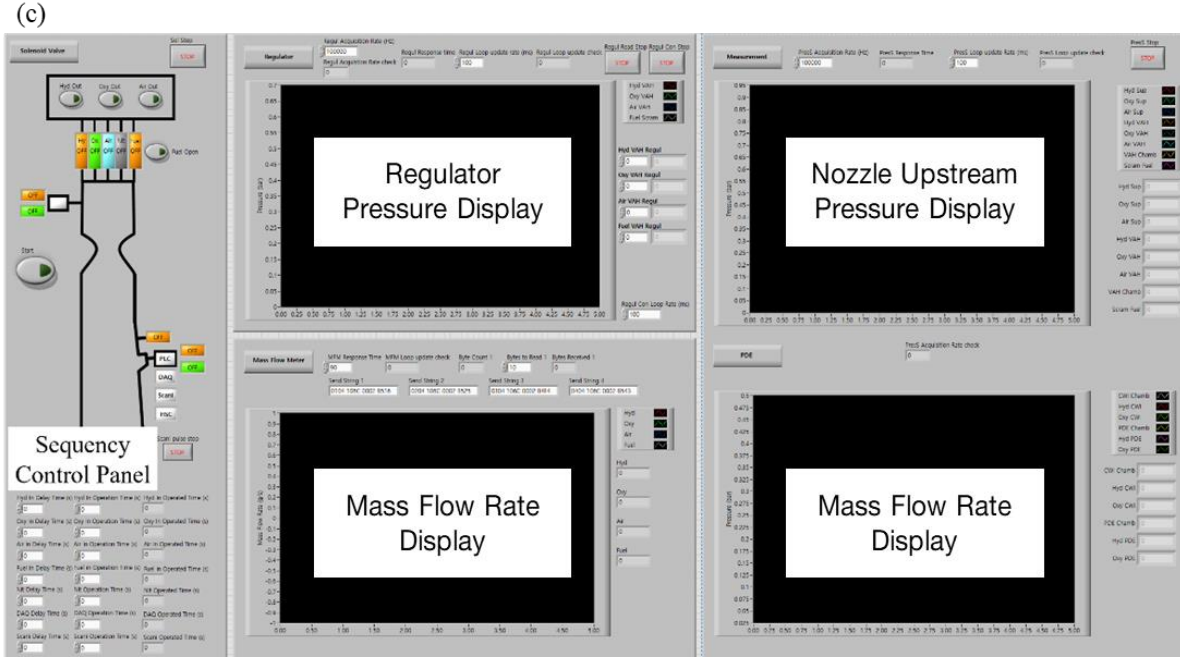


Fig 4. Monitoring and control system of the gas supply and measurement systems at Pusan National University: (a) control panel with data acquisition and gas supply modules, (b) components of the control panel, and (c) sensors and trigger control modules connected to the NI CompactRIO 9045.

Component (2), the solid-state relays, deliver control signals to actuate the pneumatic valves. Component (3) manages sensor data acquisition, valve actuation control signals, and triggering of the high-speed camera. Fig. 4(a) shows the overall control panel hardware responsible for gas supply control, sensor monitoring, and high-speed camera triggering, while Fig. 4(b) illustrates the three functional parts of the control panel. Component (1), the power supply, provides electrical power to the sensors and pneumatic valves. Component (2), the solid-state relays, transmit control signals to actuate the pneumatic valves. Finally, Component (3) manages data acquisition from the sensors, control signals for valve actuation, and triggering of the high-speed camera.

2.3. Nozzle Wedge Experimental setup

Verification of the COST nozzle exit condition was performed using the Vitiated Air Heater (VAH) facility at Pusan National University. The VAH is a rocket-type, combustion-driven, film-cooled air heater typically used for high-altitude emulations. Fig. 5 presents a schematic of the VAH directly connected to the CRST nozzle. As shown, the VAH employs a coaxial injector that combusts hydrogen and oxygen in the core region, while air is injected near the wall to provide film cooling and simultaneously generate high-temperature air[25-27]. However, in this study, emulating flight conditions was not suitable for verifying the nozzle exit Mach number, because expansion waves were generated at the exit and influenced the flow before it reached the wedge. Instead, cold-flow experiments with air only were conducted at a pressure ratio of ~7 to reproduce near-ideal expansion conditions and to verify the nozzle design for achieving Mach 2.

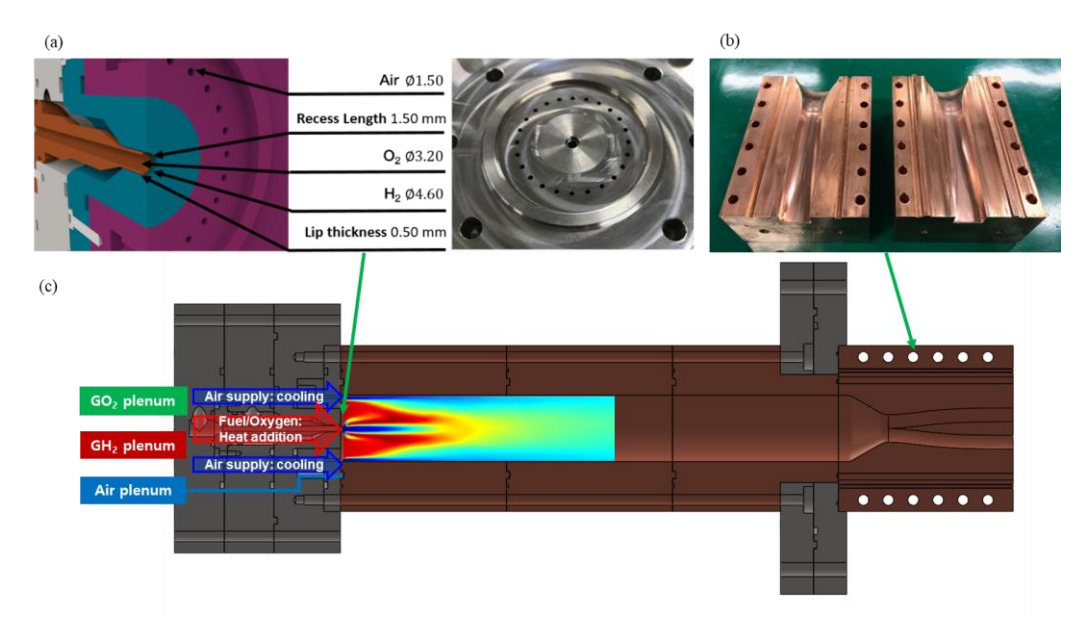


Fig 5. VAH directly connected to the COST nozzle: (a) schematic and fabricated injector, (b) fabricated COST nozzle, and (c) Cross-section of the VAH–COST nozzle configuration [7-14].



Fig 6. Experimental setup for flow uniformity measurement of the COST nozzle.

As shown in Fig. 6, the COST nozzle was directly connected to the VAH, and a wedge was installed at the nozzle exit to measure Mach number. Measurements were taken at the centerline (h = 100 mm) and at the center of the lower semicircle (h = 92 mm) (Fig. 7). These two positions were selected to compare Mach number variations with respect to h and to evaluate the degree of flow uniformity at the nozzle exit. The wedge was made of tungsten with a 20° half-angle. This material and angle were selected based on previous studies [14], which showed that they provided the greatest resistance to damage.

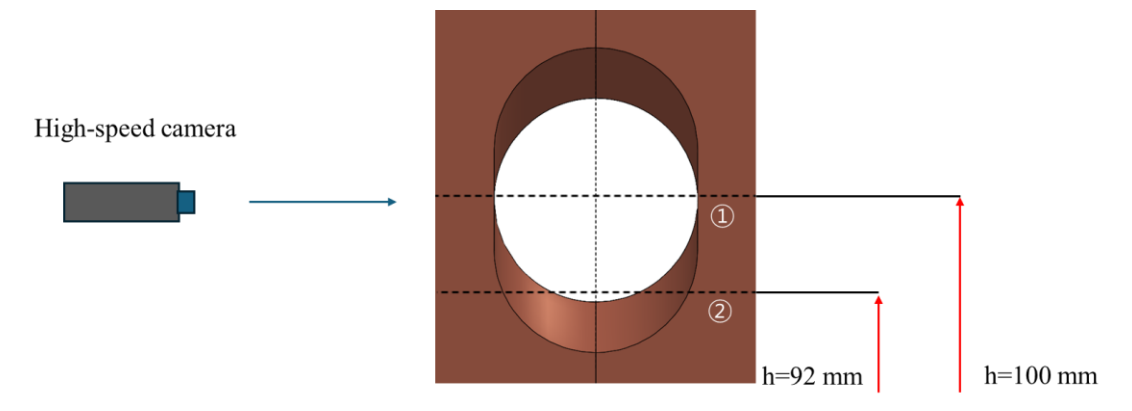


Fig 7. Schematic of flow uniformity verification experiment. h denotes the height from the testbed to the measurement point: ① h=100 mm and ② h=92 mm.

To capture the nozzle exit flow, a high-speed camera (Phantom Inc., Wayne, NJ, USA) in combination with the Schlieren technique was employed. The Schlieren method is a well-established visualization technique that detects sharp density gradients in a flow by exploiting changes in light refraction as it passes through media of varying density. In this study, a tungsten wedge was installed at the COST nozzle exit, and the shocks generated by the wedge were visualized to determine the corresponding shock angles. The imaging conditions are listed in Table 1, and Fig. 8 presents a schematic of the Schlieren technique. Averaged Schlieren images were used to confirm shock stability, and Mach numbers were calculated from the θ - β -M relation (Eq. 1). The calculation procedure was as follows:

- 1. Measure θ and β from the averaged Schlieren images obtained by the high-speed camera.
- 2. Assume $M_{calc} = 2$ and compute the θ_{calc} from the measured β using the Eq. 1.
- 3. Compare the measured θ with θ_{calc} obtained from the assumption.
- 4. If the error is within ± 0.005 , confirm the Mach number; otherwise, adjust M_{calc} and repeat from step 2.

Each experiment was repeated twice for reproducibility.

Table 1. Experimental conditions of the high-speed camera.

Resolution	Fps	Exposure time	Period
512 × 320	80000	$1~\mu s$	12.5 μs

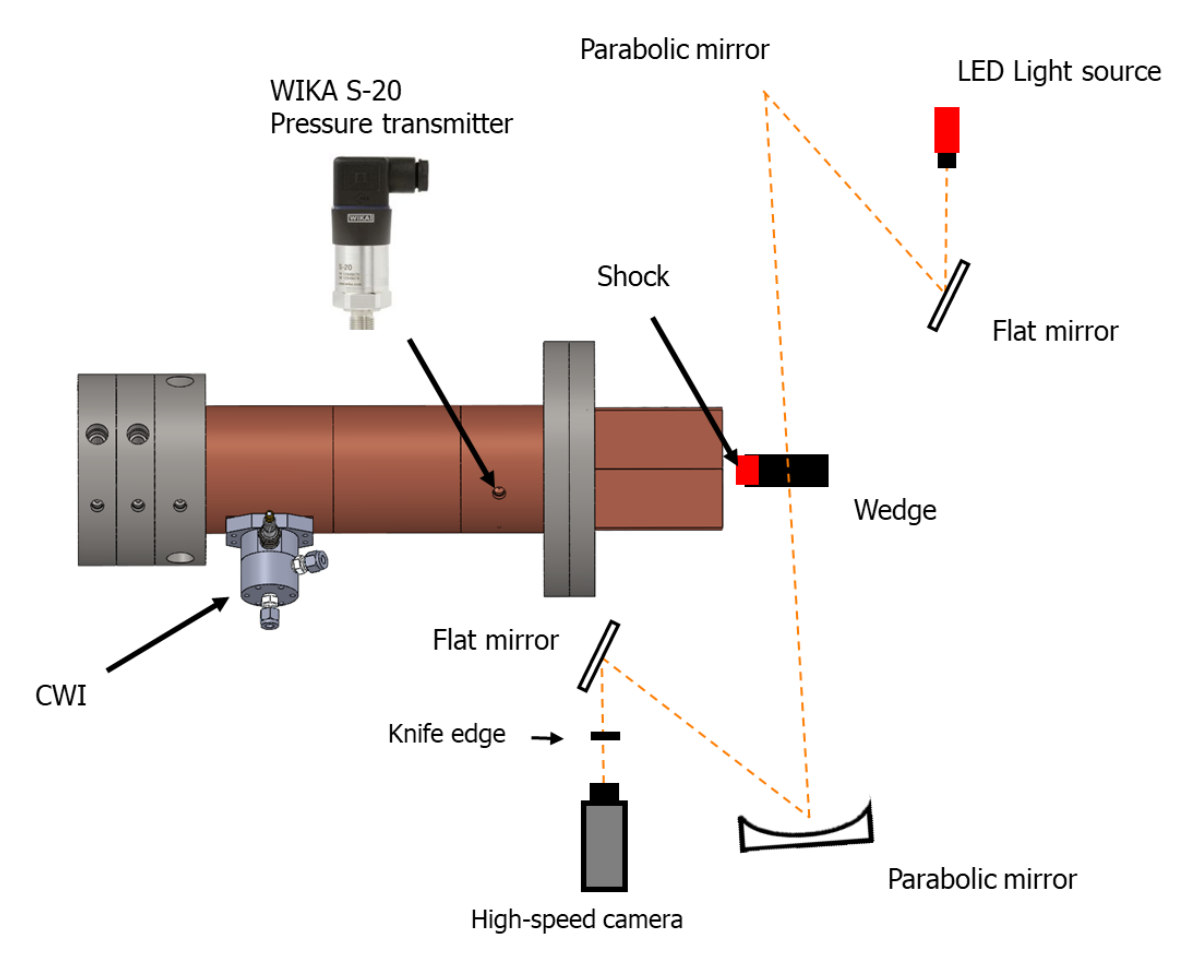


Fig 8. Schematic of the Schlieren technique and experimental setup for shock visualization.

$$tan\theta = \frac{2\cot\beta \,(M_1^2\sin^2\beta - 1)}{M_1^2(\gamma + 2\cos2\beta) + 2} \tag{1}$$

3. Nozzle Design and Flow Uniformity Verification

The results are shown in Fig. 9 and Table 2, where the averaged Schlieren images for the h100 and h92 cases are presented, and the corresponding M_{calc} , θ_{calc} , \dot{m} , and P obtained from the experiments are summarized. For the h100 case, expansion waves were observed in the upper region, so Mach number was calculated using the shock angle below the wedge. In the h92 case, the lower shock was indistinct, so the upper shock angle was used. For h100, the measured β angles were 51.97° and 50.75°, corresponding to Mach numbers of 2.045 and 2.087. For h92, the β angles were 50.91° and 50.27°, giving Mach numbers of 2.076 and 2.099. Since the measurements of θ and β angles were performed manually, errors could occur when comparing cases, such as choosing different origins for each case. To address this, the research team created a single orthogonal coordinate system by averaging the images shown in Figs. 9(a) and 9(b) and in Figs. 9(c) and 9(d). In this way, the θ and β angles were measured for each case with a common origin across the first and second experimental runs, thereby minimizing errors and further correcting for any misalignment of the wedge angle. All calculated Mach numbers were slightly higher than the design target of Mach 2, likely due to the boundary-layer correction applied in Sivell's method, which tends to overestimate the boundary-layer thickness[23]. The difference between h100 and h92 cases was only 0.012-0.031 in Mach number (<2% error), indicating nearly identical exit conditions.

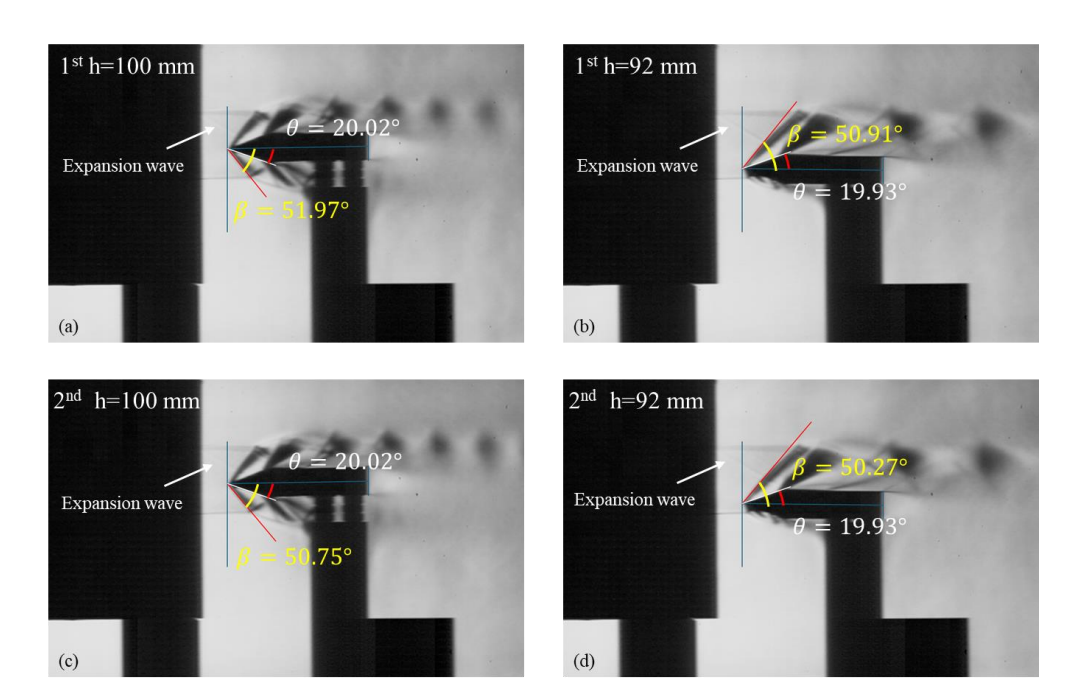


Fig 9. Averaged Schlieren images from cold-flow experiments: (a) first h100 case, (b) first h92 case, (c) second h100 case, and (d) second h92 case.

Table 2. Summarization of flow uniformity experiment result for each parameter: M_{calc} , θ_{calc} , θ and P.

Case	M_{calc}	$\theta_{ m calc}$ (°)	Θ (°)	P (bar)
1 st h100	2.045	20.017	20.02	6.995
1 st h92	2.076	19.936	19.93	7.01
2 nd h100	2.087	20.019	20.02	6.999
2 nd h92	2.099	19.929	19.93	6.987

4. Conclusion

Despite the more complex design and fabrication, the obround scramjet configuration shows strong potential as an alternative cross-section by combining the favorable flow characteristics of axisymmetric and rectangular scramjets. In particular, the obround geometry is expected to alleviate corner-induced pressure losses commonly observed in rectangular combustors, while at the same time offering advantages for flow visualization and experimental accessibility.

In this study, the COST nozzle was designed as a preliminary step toward investigating the fundamental flow characteristics of the obround scramjet. The nozzle design incorporated boundary-layer corrections using Sivell's method and was verified through cold-flow experiments employing high-speed Schlieren imaging with wedge diagnostics. The results indicated that the exit flow condition closely matched the target Mach number of 2, with only a minor deviation attributable to boundary-layer correction effects. Furthermore, the near-uniform Mach numbers measured at two different nozzle exit positions confirmed the flow uniformity and reliability of the COST nozzle.

These findings validate the feasibility of using a COST nozzle to reproduce the desired isolator inlet conditions, thereby establishing a solid foundation for subsequent investigations of isolator and combustor flow behavior in obround scramjets. Future research will extend these efforts to include hot-fire experiments and numerical analyses, enabling comprehensive evaluation of combustion performance and stability in obround cross-section scramjets.

References

- 1. Lee, G.S.; Baccarella, D.; Liu, Q.; Elliott, G.S.; Lee, T. Pseudoshock dimensionality in axisymmetric and rectangular scramjets. In Proceedings of the AIAA Scitech 2020 Forum, 2020; p. 1610.
- 2. Lee, G.S. A combined cycle approach to dual-mode scramjet design and analysis. University of Illinois Urbana-Champaign, 2023.
- 3. Yentsch, R.J.; Gaitonde, D.V. Comparison of mode-transition phenomena in axisymmetric and rectangular scramjet flowpaths. In Proceedings of the 52nd Aerospace Sciences Meeting, 2014; p. 0625.
- 4. Sharath, S.; Jana, T.; Kaushik, M. Shock-Wave/Boundary-Layer Interactions in Scramjet Intakes with Axisymmetric and Planar Isolators. *Advances in Astronautics Science and Technology* **2023**, *6*, 133-142.
- 5. Choi, J.-Y.; Jeung, I.-S.; Yoon, Y. Scaling effect of the combustion induced by shock-wave boundary-layer interaction in premixed gas. In Proceedings of the Symposium (International) on Combustion, 1998; pp. 2181-2188.
- 6. Choi, J.; Noh, J.; Byun, J.-R.; Lim, J.-S.; Togai, K.; Yang, V. Numerical investigation of combustion/shock-train interactions in a dual-mode scramjet engine. In Proceedings of the 17th AIAA International Space Planes and Hypersonic Systems and Technologies Conference, 2011; p. 2395.
- 7. Choi, J.-Y.; Ma, F.; Yang, V. Dynamic combustion characteristics in scramjet combustors with transverse fuel injection. In Proceedings of the 41st AIAA/ASME/SAE/ASEE Joint Propulsion Conference & Exhibit, 2005; p. 4428.
- 8. Won, S.-H.; Jeung, I.-S.; Choi, J.-Y. Turbulent combustion characteristics in HyShot model combustor with transverse fuel injection. In Proceedings of the 43rd AIAA/ASME/SAE/ASEE Joint Propulsion Conference & Exhibit, 2007; p. 5427.
- 9. Choi, J.-Y.; Ma, F.; Yang, V.; Won, S.-H.; Jeung, I.-S. Detached Eddy simulation of combustion dynamics in scramjet combustors. In Proceedings of the 43rd AIAA/ASME/SAE/ASEE Joint Propulsion Conference & Exhibit, 2007; p. 5027.
- 10. Vyasaprasath, K.; Oh, S.; Kim, K.-S.; Choi, J.-Y. Numerical studies of supersonic planar mixing and turbulent combustion using a detached eddy simulation (DES) model. *International Journal of Aeronautical and Space Sciences* **2015**, *16*, 560-570.
- 11. Jeong, S.-M.; Lee, J.-H.; Choi, J.-Y. Numerical investigation of low-frequency instability and frequency shifting in a scramjet combustor. *Proceedings of the Combustion Institute* **2023**, *39*, 3107-3116.
- 12. Jeong, S.-M.; Choi, J.-Y. Combined diagnostic analysis of dynamic combustion characteristics in a scramjet engine. *Energies* **2020**, *13*, 4029.
- 13. Kim, H.-S.; Oh, S.; Choi, J.-Y. Quasi-1D analysis and performance estimation of a sub-scale RBCC engine with chemical equilibrium. *Aerospace Science and Technology* **2017**, *69*, 39-47.
- 14. Choi, J.-Y.; Jeung, I.-S.; Yoon, Y. Unsteady-state simulation of model ram accelerator in expansion tube. *AIAA journal* **1999**, *37*, 537-543.
- 15. Choi, J.-Y.; Unnikrishnan, U.; Hwang, W.-S.; Jeong, S.-M.; Han, S.-H.; Kim, K.H.; Yang, V. Effect of fuel temperature on flame characteristics of supersonic turbulent combustion. *Fuel* **2022**, *329*, 125310.
- 16. Shin, E.; Won, S.; Cho, D.-R.; Choi, J.-Y. Hybrid RANS/LES study of base-bleed flows in supersonic mainstream. In Proceedings of the 15th AIAA International Space Planes and Hypersonic Systems and Technologies Conference, 2008; p. 2588.
- 17. Choi, J.; Kim, K.H.; Han, S. High resolution numerical study on the coaxial supersonic turbulent flame structures. In Proceedings of the 50th AIAA/ASME/SAE/ASEE Joint Propulsion Conference, 2014; p. 3745.
- 18. Kato, N.; Lee, G.S.; Lee, T. A Comparison Between Axisymmetric and Perisymmetric Scramjet Flowpaths. In Proceedings of the AIAA SCITECH 2022 Forum, 2022; p. 1409.
- 19. Yao, W.; Yuan, Y.; Li, X.; Wang, J.; Wu, K.; Fan, X. Comparative study of elliptic and round scramjet combustors fueled by RP-3. *Journal of Propulsion and Power* **2018**, *34*, 772-786.
- 20. Kim, M.-S.; Koo, I.-H.; Lee, K.-H.; Lee, E.-S.; Han, H.-S.; Jeong, S.-M.; Kim, H.; Choi, J.-Y. Experimental study on the ignition characteristics of scramjet combustor with tandem cavities using micro-pulse detonation engine. *Aerospace* **2023**, *10*, 706.

- 21. Kim, M.-S.; Sung, B.-K.; Lee, K.-H.; Jeong, S.-M.; Choi, J.-Y.; Yu, K.H. Experimental DMD analysis of combustion modes and instabilities in a scramjet combustor. *Aerospace Science and Technology* **2025**, *157*, 109783.
- 22. Sung, B.-K.; Choi, J.-Y. Design of a Mach 2 shape transition nozzle for lab-scale direct-connect supersonic combustor. *Aerospace Science and Technology* **2021**, *117*, 106906, doi:https://doi.org/10.1016/j.ast.2021.106906.
- 23. Sung, B.-K.; Jeong, S.-M.; Choi, J.-Y. Direct-connect supersonic nozzle design considering the effect of combustion. *Aerospace Science and Technology* **2023**, *133*, 108094.
- 24. Lee, K.-H.; Kim, M.-S.; Choi, J.-Y.; Yu, K.H. An Experimental Investigation of Low-Frequency Active Excitation in Scramjet Combustor Using a Micro-Pulse Detonation Engine. *Aerospace (MDPI Publishing)* **2024**, *11*.
- 25. Jeong, S.-M.; Han, H.-S.; Sung, B.-K.; Kim, W.; Choi, J.-Y. Reactive flow dynamics of low-frequency instability in a scramjet combustor. *Aerospace* **2023**, *10*, 932.
- 26. Jeong, S.-M.; Kim, J.-E.; Kim, M.-S.; Sung, B.-K.; Choi, J.-Y.; Yu, K.H. Numerical study on the combustion characteristics and performances of single and multi-injectors in a scramjet combustor. *Aerospace Science and Technology* **2024**, *155*, 109697.
- 27. Lee, J.-H.; Lee, E.-S.; Han, H.-S.; Kim, M.-S.; Choi, J.-Y. A study on a vitiated air heater for a direct-connect scramjet combustor and preliminary test on the scramjet combustor ignition. *Aerospace* **2023**, *10*, 415.